Climate Dynamics (1996) 12:711–721

Climate Dynamics

© Springer-Verlag 1996

Future ocean uptake of CO_2: interaction between ocean circulation and biology

Ernst Maier-Reimer, Uwe Mikolajewicz, Arne Winguth

Max-Planck Institut für Meteorologie, D-20146 Hamburg, Germany

Received: 9 August 1995 / Accepted: 22 April 1996

Abstract. We discuss the potential variations of the biological pump that can be expected from a change in the oceanic circulation in the ongoing global warming. The biogeochemical model is based on the assumption of a perfect stoichiometric composition (Redfield ratios) of organic material. Upwelling nutrients are transformed into organic particles that sink to the deep ocean according to observed profiles. The physical circulation model is driven by the warming pattern as derived from scenario computations of a fully coupled ocean-atmosphere model. The amplitude of the warming is determined from the varying concentration of atmospheric CO_2. The model predicts a pronounced weakening of the thermohaline overturning. This is connected with a reduction of the transient uptake capacity of the ocean. It yields also a more effective removal of organic material from the surface which partly compensates the physical effects of solubility. Both effects are rather marginal for the evolution of atmospheric pCO_2. Running climate models and carbon cycle models separately seems to be justified.

1 Introduction

The increase of CO_2 concentrations in the atmosphere due to the combustion of fossil fuels has stimulated (Revelle and Suess 1957) a broad spectrum of research. One key question concerns the amount of excess CO_2 that can be absorbed by the oceans. The combination of elementary inorganic chemistry of sea water with the oceanic volume gives an upper estimate of 5/6 (ignoring sediment) for the storage capacity of the oceans, as already pointed out by Arrhenius at the end of the last century (Revelle 1985). Yet because the deep ocean circulates slowly, this asymptotic value may be reached only after several thousand years circulation. At present, approximately one third of CO_2 emissions enter the ocean (Houghton et al. 1990), an estimate that represents a compromise between ocean model studies and estimates from direct atmospheric observations.

Simplified box models to study the oceanic CO_2 uptake were developed already 20 years ago (e.g. Oeschger et al. 1975). More recently, three-dimensional circulation models have been used for such studies (Maier-Reimer and Hasselmann 1987; Sarmiento et al. 1992). Their results more or less confirm the previous estimates of global CO_2-uptake.

Several pumping mechanisms have been identified to explain the observed vertical gradient in the distribution of carbon in the ocean (Volk and Hoffert 1985: Broecker and Peng 1986). The most obvious process is provided by the high solubility of CO_2 at low temperatures. This mechanism is called the solubility pump. Two other processes termed biological pumps are caused by the formation of soft tissue matter (soft tissue pump) and of calcium carbonate (calcium carbonate pump) with opposing effects on the partial pressure pCO_2. All three have their counterparts provided by low latitude heating, remineralization, and dissolution, respectively. The deep waters of the ocean are cold, but the products of deep remineralization processes increase the local pCO_2 substantially above the values of cold surface waters.

In the past, the main shortcoming of three dimensional models (apart from an insufficient formation of North Atlantic deep water see e.g. Maier-Reimer and Hasselmann 1987) was the complete neglect of all biological processes. Vertical gradients of the sum of the species CO_2, H_2CO_3, HCO_3^-, and CO_3^- which is also known as TIC or DIC (total or dissolved inorganic carbon) or ΣCO_2 are largely due to biological processes; thermodynamical effects alone explain only about one quarter of the observed gradients (Maier-Reimer and Hasselmann 1987). Without the effects due to biology, the ocean would be chemically quite different. Consequently, without biology the basic state upon which the anthropogenic perturbation is imposed, cannot be compared with the distribution of CO_2 in the real ocean.

Correspondence to: E. Maier-Reimer

The role of biological processes in the uptake of fossil fuel CO_2 by the ocean is often misinterpreted. The notion that ocean biology is responsible for a net transfer of excess CO_2 from the atmosphere to the deep ocean is in striking contradiction to the fact that the CO_2 content of the atmosphere has remained essentially constant during the 10000 years preceding the onset of anthropogenic emissions (Neftel et al. 1982). The ongoing sedimentation of calcium carbonate at the sea floor and of organic matter on some shelf areas are roughly in balance with river inputs and terrestrial modification, regarding the effects on atmospheric pCO_2. More quantitative arguments against the role of biology in the sequestering of additional CO_2 are given by Broecker (1991). The natural biological pump is roughly in equilibrium with the upwelling products of the inverse processes (nutrient remineralization and calcite dissolution). In regions of high productivity, the DIC content of the surface water is depleted by only 15% of the deep sea value. It is difficult to imagine that a 10% increase of dissolved CO_2 (the increase that would be in equilibrium with a doubling in the atmosphere (Revelle and Suess 1957)) could substantially improve the utilization of nutrients. On the other hand, some diatom species depend on neutral aqueous CO_2 whose contribution to the total dissolved CO_2 is in the order of 1% only. Riebesell et al. (1993) have indeed shown in laboratory experiments that under optimal growth conditions a reduction of CO_2 slows the cell doubling rate. They did not show, however, a pronounced increase in the growth rate under artificially enhanced pCO_2 nor did they show any changes in the carbon fixation per nutrient unit (Wolf-Gladrow 1994).

Working in the opposite direction, a positive feedback of marine biology to the CO_2-induced global warming has been identified by Frankignoulle et al. (1994) since in warmer waters there is a higher likelihood for calcareous-forming algae to develop. The corresponding removal of alkalinity would tend to increase the atmospheric pCO_2.

Additionally, biology indirectly affects the uptake of fossil fuel CO_2, because the upper 10 to 20 cm of the sediment are bioturbated. Thus, they remain in close contact with the overlying water. Incidentally, this pool is estimated to contain the same amount of carbon in the form of $CaCO_3$ as the present estimates of coal resources (Broecker and Takahashi 1977). During the uptake of excess CO_2 the surface water becomes more acidic. When it gains contact with sediments, the additional acidity and, thus, the excess CO_2 tends to be neutralized by the dissolution of $CaCO_3$. In the modern ocean, carbonate sediments are preserved, at least for the global average, at depths shallower than 4 km. In equilibrium with a doubled CO_2 content in the atmosphere, the concentration of carbonate ions in the seawater will be halved and the calcite preservation level (lysocline) will rise considerably (up to a few kilometers in the Atlantic) and thus expose the corresponding sediment layers to dissolution. The result of sediment dissolution on the atmospheric pCO_2 seems a paradox, caused by the fact that with the dissolution of $CaCO_3$ double the amount of alkalinity is added to the system. Figure 1 shows the response of atmospheric pCO_2 of different versions of the HAMOCC (Hamburg model of oceanic carbon cycle) to a sudden doubling of atmospheric pCO_2. The inorganic version (Maier-Reimer and Hasselmann 1987) and the first order biota version without the interactive sediment pool (Bacastow and Maier-Reimer 1990) behave similarly despite the completely different structure of ΣCO_2 in the undisturbed state. In both models, the inventories of alkalinity were fixed to yield a preindustrial atmospheric pCO_2 of 278 ppm. With the assumption of a constant carbon to nutrient (Redfield) ratio, the behaviour should be to first order identical. Response curves diverge only within the width of the bold line in Fig. 1, due to the nonlinearity of the inorganic chemistry. The inclusion of an interactive sediment pool (Heinze et al. 1991) modifies the uptake characteristics substantially after a few centuries. The figure also displays the response of one of the simplified models (Siegenthaler 1983), the model having incidently the highest CO_2 uptake rate.

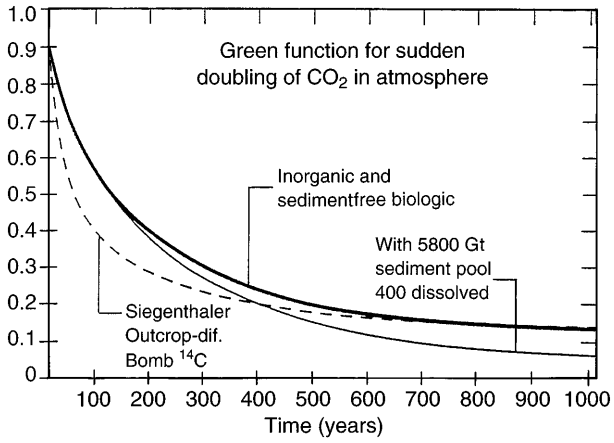

Fig. 1. Response of the atmospheric CO_2 concentration on a sudden doubling for different versions of the HAMOCC model and for one of Siegenthaler's (1983) models (with the highest uptake rate). Since no explicit fertilization by excess carbon is assumed, the response of the inorganic model and the sediment-free model are almost identical

A direct effect of the biological pump on the uptake of CO_2 can be expected only from changes in the pumping strength. Such changes could stem from changes in the plankton communities as a result of changes in thermodynamic surface properties or from a change in the residence time of particulate matter in the deep ocean (see Heinze et al. 1991).

So far, predictions concerning future CO_2 concentrations as a result of prescribed emissions have been made with carbon cycle models alone (at least 3-D models), where the oceanic circulation was kept constant. The resulting predictions of future greenhouse gas concentrations were used to force coupled OAGCMs which gave an estimate of future climate changes. These experimemts show a marked response

of the thermohaline circulation in response to the prescribed increase in atmospheric concentrations of greenhouse gases (e.g. Manabe et al. 1991; Cubasch et al. 1992; for a review see Gates et al. 1992). Manabe and Stouffer (1994) showed a permanent reduction of NADW formation in case of a quadrupling of atmospheric CO_2 concentrations. It has been speculated whether these changes in ocean circulation might affect the oceanic uptake of CO_2 and, thus, constitute a positive feedback for the atmospheric greenhouse gas concentrations. Several potential ways of influencing the oceanic uptake rates are possible. In addition to changes in the biological pump, changes in the solubility due to changes in SST and the reduced ventilation of the deep ocean are candidates for potential feedback mechanisms.

In view of the inability to explain the glacial-interglacial variations of atmospheric pCO_2 by carbon cycle models in stationary states with fixed tracer inventories (e.g. Heinze et al. 1991), it is expected that the feedback of the changing oceanic circulation on the atmospheric concentration of CO_2 is small. Sanyal et al. (1995) pointed out that a possible decrease of the atmospheric CO_2 level during the last glacial maximum could have been caused by an increased ratio of organic carbon to carbonate in the 'rain' to the sea floor, which led to an increase in carbonate ion concentration and pH of deep water without a corresponding increase in the lysocline depth. However, carbon cycle models including a transient state could be able to show more substantial excursions of atmospheric pCO_2 (Archer and Maier-Reimer 1994).

The most complete way of investigating the role of feedbacks between greenhouse gas induced climate changes and the subsequent changes in the oceanic uptake of CO_2 due to these circulation changes and the resulting changes in atmospheric CO_2 concentrations would be to couple a coupled OAGCM with an ocean carbon cycle model. This approach, however, would cause many problems, since it would imply the computationally ineffective combination of the huge memory requirements of the carbon cycle model with the huge CPU-time requirements of the atmosphere model. Additional problems would be due to the long time-constants in the carbon cycle, especially from the processes involving sediment. A model that includes these processes requires a much longer spinup integration. Thus, the problems due to climate drift after insufficiently long spinup would become much worse.

The experiment of Mikolajewicz et al. (1990) with an uncoupled OGCM in response to a prescribed global warming in the atmosphere was able to capture the most important features of the response in coupled OAGCMs, at least in a qualitative way. They were able to show a marked reduction in the ventilation of the deep ocean and were even able to reproduce the minimum of the warming in the northern North Atlantic which shows up in all coupled models (see Gates et al. 1992 for a review). Thus, to avoid the problems involved with the coupled models, we will try in this study to assess the role of potential feedbacks due to changes in the physical state of the ocean caused by greenhouse gas induced warming during the next century in experiments with the Hamburg model of the oceanic carbon cycle (HAMOCC3, Maier-Reimer 1993), coupled online to the LSG ocean general circulation model (OGCM) (Maier-Reimer et al. 1993) together with a simple atmospheric feedback derived from a coupled OAGCM. Changes in atmospheric CO_2 concentrations are directly transferred into a radiative forcing for the physical part of the model.

We look for the increase of atmospheric pCO_2 resulting from a prescribed high emission scenario. We compare the results from an experiment where the ocean circulation is allowed to change through time in response to a prescribed greenhouse gas emission scenario with the results from an experiment corresponding to traditional CO_2 uptake experiments with constant ocean circulation (like Maier-Reimer and Hasselmann 1987, or Sarmiento et al. 1992). The experiment with time varying ocean circulation can be taken as a first order guess for the feedbacks that could be expected when ocean, atmosphere, and marine carbon cycle models were coupled online.

This study is organized as follows: the model and the applied feedback are described in Sect. 2. In Sect. 3 sensitivity experiments are presented highlighting the role of the thermohaline circulation, the biological productivity and a complete sedimentation of the biological export production. In Sect. 4 the effect of time varying ocean circulation due to global warming on the oceanic uptake of anthropogenic CO_2 is discussed. Final conclusions are given at the end of the study. A list of all experiments discussed in this work is given in Table 1.

2 The model

2.1 The ocean circulation model

We use the 11 layer version ATOS1 of the Hamburg LSG general circulation model as described by Maier-Reimer et al. (1993). This version has been defined from a series of experiments with different boundary conditions to represent the standard LSG control run. The main criterion for the choice was the realistic reproduction of natural radiocarbon in the Atlantic which is a sensitive variable for the conveyor belt structure (Broecker 1991) of the circulation model. The thermodynamic variables and the horizontal components of velocity are defined at depth levels 25, 75, 150, 250, 450, 700, 1000, 2000, 3000, 4000, and 5000 m. The layer thickness is normally defined by the computation levels: however, at locations where the assumed topography intersects the levels of computation, a modified layer thickness is introduced in order to obtain smoother variations of depth than could otherwise be achieved for the low number of levels. From this run the freshwater fluxes resulting from the relaxation to the climatological sea surface salinity were analyzed

Table 1. Overview of the 5 sensitivity experiments: 3 experiments to study the role of the biological pump, no circulation (NOCIRC), no biology (NOBIO), and perfect sedimentation (PERSED). Two experiments to study the effect on the carbon cycle due to an atmospheric CO_2 feedback and change in the ocean circulation caused by an anthropogenic CO_2 emission from 1750 to 2100 (FEED with feedback and NOFEED without feedback; for details see text)

	Stopped circulation	Killed biology	Perfect sedimentation	Anthropogenic CO_2 emission	CO_2 feedback
CTRL					
NOCIRC	×				
NOBIO		×			
PERSED			×		
NOFFED				×	
FEED				×	×

and used as a forcing for the second part of the spinup under tradional mixed boundary conditons (restoring condition at the surface for temperature, flux condition for salinity). The model was run with this type of boundary condition until a steady state has been reached. This spinup has also been used in a number of sensitivity experiments (e.g. Mikolajewicz et al. 1990).

One of the most striking features of coupled ocean-atmosphere models is a transient pronounced cooling of several ocean regions, especially at locations where deep water is formed (Cubasch et al. 1992; Manabe et. al. 1991). These exceptions from the global warming trend are also found in analyses of historical data sets from the past 50 years (Jones et al. 1986). Mikolajewicz et al. (1990) discussed an experiment in which the Hamburg LSG model was driven under mixed boundary conditions with the mean equilibrium warming pattern as predicted from four different AGCMs, coupled to mixed layer ocean models, for the case of a doubling of CO_2. They have shown with an ocean only model that such a cooling may be explained by oceanic processes alone. It is due to the effect that a reduction of deepwater formation weakens the deep flow towards the equator and, thus, reduces the supply of warm water towards the pole. A potential feedback of the SST on the forcing atmospheric temperature was ignored in that experiment. This neglect of a feedback, however, has been identified as a major shortcoming of traditional mixed boundary conditions. From a series of recent papers (e.g. Wright and Stocker 1993; Zhang et al. 1993; Mikolajewicz and Maier-Reimer 1994; Rahmstorf 1994) it has been concluded that the traditional form of the mixed boundary strongly tends to produce unrealistically high senstitivity of the thermohaline circulation to perturbations, we followed the approach of Mikolajewicz and Maier-Reimer (1994) and chose a combination of heat flux forcing together with a weak restoring of the surface temperature (16 $Wm^{-2}K^{-1}$). This value turned out to give reasonable sensitivities of the thermohaline circulation to perturbations. We made an additional step in the spinup with the heat fluxes analyzed from the spinup with mixed boundary conditions. This is identical to the spinup used in Mikolajewicz and Maier-Reimer (1994). The state achieved at the end of this spinup will serve as control run (CTRL) for the rest of this study.

2.2 The atmospheric feedback

The deviations of the atmospheric CO_2 concentrations from the steady state of the model (276.7 ppm, experiment CTRL) are transferred into a radiative forcing for the ocean by a logarithmic law

$$F_{HCO_2}(t) = \alpha \ln(pCO_2(t)/276.7 \text{ ppm})$$

with a radiative forcing constant α and $pCO_2(t)$ the atmospheric CO_2 partial pressure at time t. This equation alone is not sufficient, there needs to be a damping of the resulting increase in SSTs. The warming pattern was taken from the experiments of Cubasch et al. (1994). They made four 50 y integrations starting from a state corresponding to the radiative conditions of 1985 with IPCC "business as usual" scenario A. The four experiments differed only in the choice of the initial conditions. With this approach it is possible to eliminate the effect of natural variability of the atmosphere-ocean system from the greenhouse signal, provided enough realizations are available. Due to the high costs only four runs could be made, which significantly reduces the noise in the estimate of the signal compared to a single integration, but the sample size is definitely too small to eliminate it totally. The monthly climatological warming pattern was derived from the response in near-surface air temperature averaged over the last decade of all experiments. The annual mean of this warming pattern is shown in Fig. 2. The dominant feature is the stronger warming over land than over oceans due to the thermal inertia of the ocean. The weak cooling in the North Atlantic is associated with the reduction of the formation of NADW. The strong signals in the Southern Ocean are due to large changes in sea ice coverage and changes in the location of AABW formation.

This pattern is multiplied by a variable amplitude. The amplitude is a function of the global mean SST change of the ocean model. To allow a damping effect, the resulting amplitude of change in air temperature is only 90% of the SST change. This field is added to the present climatological surface air temperature derived from the COADS data set and used as restoring temperature field for the SSTs. Together with a value of α for the radiative forcing of 5 $Wm^{-2}K^{-1}$ this gives a climate sensitivity in global mean SST of 3.2 °C for

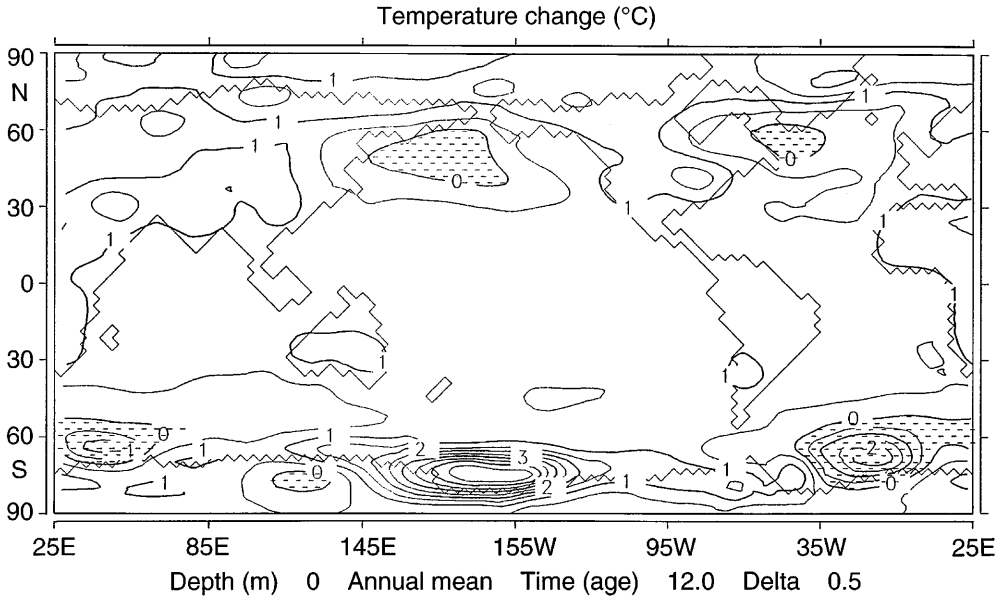

Fig. 2. Structure of the annual mean atmospheric temperature response as derived from the final decade of four 50 y-integrations with IPCC "business as usual" scenario A in the ECHAM1/LSG coupled OAGCM (data from Cubasch et al. 1994). Contour interval is 0.5 K. *Areas* of cooling are *stippled*

CO_2-doubling. Both the damping constant for the global mean SST and the radiative forcing were chosen to give a best fit to the coupled experiments described in Cubasch et al. (1994). The choice of the damping coefficient also determines the response time scales of the present model. A fit of exponential functions $(1-\exp\{-t/\tau\})$ (see Hasselmann et al. 1993 for details of the procedure) to a time series of the response of the global mean SST to an instantaneous doubling of atmospheric CO_2 concentrations requires two time constants τ: 7 years (with an amplitude of 1 °C) and 83 years (with an amplitude of 2.1 °C).

2.3 The ocean carbon cycle model

The Hamburg Ocean model of Carbon Cycle (HAMOCC3, Maier-Reimer 1993) coupled on line to the LSG-OGCM is similar to the model which was used by Winguth et al. (1994) to study ENSO-related fluctuation of the marine carbon cycle.

As described in Maier-Reimer (1993), the biological part of the carbon cycle component (HAMOCC3) of the coupled model is based on the assumption of perfect stoichiometric relationships (Redfield ratios) of organic material:

$$\delta P:\delta N:\delta C:\delta O_2 = 1:16:122:-172$$

Export production is modeled by simple Michaelis-Menten kinetics, using a basic time constant for production in optimal growth conditions which is locally modified by inhibition factors like lack of light, temperature, convective mixing, and wind stirring. Phosphate is assumed to be the one limiting nutrient; the Redfield ratio for nitrogen is used only in the determination of alkalinity changes by new production. The basic time constant of 4 months was tuned to yield realistic gradients of surface phosphate. The model predicts also production of calcareous shells, depending on the locally available silicate which is preferentially consumed; the globally averaged rain ratio $C_{calc}:C_{org}$ $(=0.17)$ was tuned to yield a realistic structure of the lysocline. In the eastern equatorial Pacific, the production is clearly overestimated, partly caused by the mismatch between the equatorial upwelling velocity and the assumed restoring time constant. The underestimation of the horizontal export of the nutrients leads to "nutrient trapping" (Najjar et al. 1992) (i.e. a positive feedback mechanism whereby strong upwelling produces strong export production that results, after remineralization, in enhanced nutrient concentrations in the upwelling water and thus further amplifies the export production). This apparent model flaw is manifested in a large subsurface pool of POC in the order of 300 GtC that cannot be remineralized due to lack of oxygen.

With the physical boundary conditions described, the coupled model was run for 10000 y to a steady state. The state at the end of the spinup serves as reference state for all other experiments and will be referenced as CTRL through the rest of this work. All other experiments were started from the final steady state of the spinup.

3 Sensitivity experiments to the role of biology

To elucidate the danger of premature conclusions from variations in the global export production, we first discuss three extreme experiments as unrealistic extrapolations of the expected changes: It is expected that the global thermohaline circulation will be reduced. We performed one experiment in which all currents are set to zero and all convection events are ignored (NOCIRC, no circulation). In this scenario, the surface

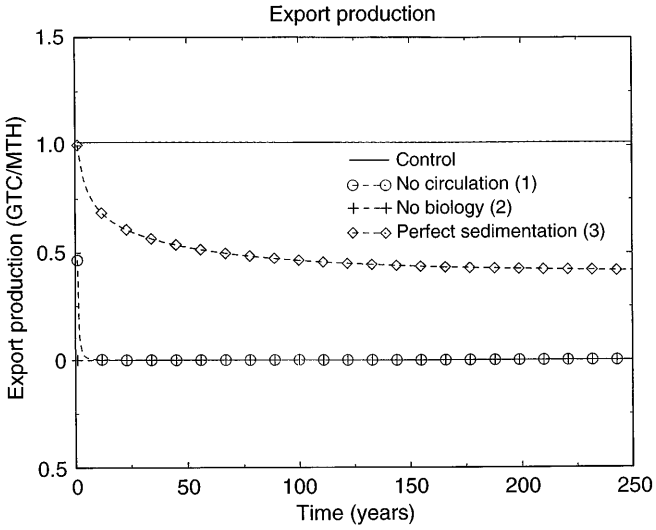

Fig. 3. Time series of the global export production for the three scenarios to study the role of the biological pump and for the control run

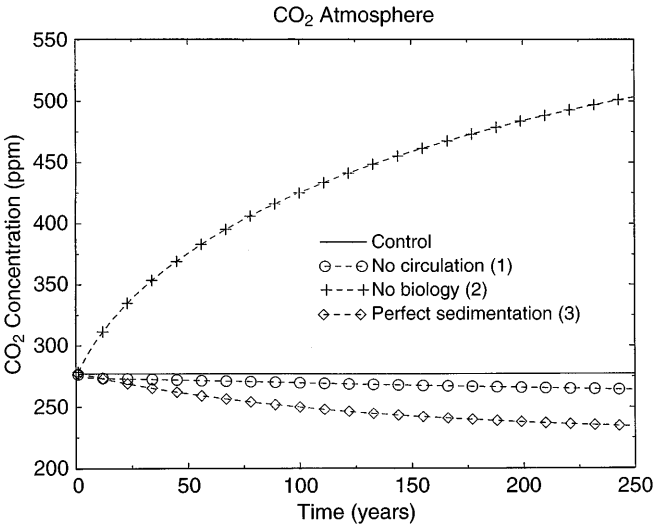

Fig. 4. Time series of the pCO_2 for the same experiments as in Fig. 3

ocean will soon be completely depleted of nutrients and the biological pump is brought to zero (Fig. 3). After 250 years integration the pCO_2 is reduced by 5% or 13 ppm (Fig. 4), which is only half of the value gained by the NADW-reduced experiment of Heinze et al. (1991). The difference between the NADW-reduced and the NOCIRC experiment can be explained by differences in the mixing of carbon and nutrient rich water from deeper levels to the surface. In the latter experiment, this mixing has been suppressed completely. This process, which tends to lower the atmospheric pCO_2 is compensated by a reduction of the biological pump which causes an increase of the pCO_2.

The increase of incoming UV-B radiation to the earths surface by ozone depletion has stimulated a discussion about the impact of photosynthesis inhibition on the global carbon budget (Häder 1993). We performed an experiment in which the biological productivity was set to zero (NOBIO, no biology). The atmospheric pCO_2 increases dramatically and reaches after 250 years integration about 2.4 times its original value (Fig. 4). After some centuries, the distribution of nutrients and the high ΣCO_2 values of the deep ocean is almost homogeneous, because due to the lack of export production no gradients can be maintained except those resulting from the temperature-dependent solubility of CO_2. Mixing of the deep sea ΣCO_2 with relatively higher concentrations in the surface layer increases the carbon content of the surface layer and hence leads to a rise of the atmospheric CO_2 level. The enhanced acidity is acting to dissolve sediments but its effect on atmospheric pCO_2 would be seen much later.

In a third experiment we artificially enhanced the effectivity of the biological pump by the assumption of complete transfer of all the material removed from the surface by export production (PERSED, perfect exposure to sedimentation) to the bottom layer. This is equivalent to a removal of all nutrients together with dissolved carbon and alkalinity according to the Redfield ratio. The resulting drop of the atmospheric pCO_2 by only 43 ppm (after 250 years integration, Fig. 4) is relatively small, only about 2% of the approximately 4000 Gt of carbon fixation that would correspond to the existing pool of phosphate. After 250 years of integration the export production is reduced by about 58% of its original value (Fig. 3). In experiments NOBIO and PERSED the surface layer is depleted by phosphate. The global average surface concentration of PO_4 is 0.5 μ mol/kg, corresponding to 60 μ mol/kg of DIC which, under preindustrial conditions, involves a drop of 60 ppm of pCO_2. In experiment NOBIO this happens only in the first layer of the model which is subsequently filled up from the atmosphere, whereas in experiment PERSED the upper thermocline as a whole is depleted providing a larger volume of water to equilibrate with the atmosphere.

These experiments indicate, however, also a second order direct effect of marine biology on the uptake of CO_2. Since the chemical state of surface water is substantially changed, the uptake capacity as defined by the buffer factor is modified. Figure 5 displays the zonally averaged differential buffer factor (Maier-Reimer and Hasselman 1987)

$$\xi = dpCO_2/d\Sigma CO_2\ (\partial pCO_2/\partial \Sigma CO_2)^{-1}$$

for year 250 of the three experiments and the control run. The higher the buffer factor, the higher is the airborne fraction of a fixed amount of CO_2-injection into the atmosphere. Since the buffer factor increases (at a given alkalinity) with increasing pCO_2 levels in atmosphere and ocean (Bacastow 1981), the experiments with a stronger biological pump imply, indeed, a slightly enhanced uptake of CO_2 by the ocean.

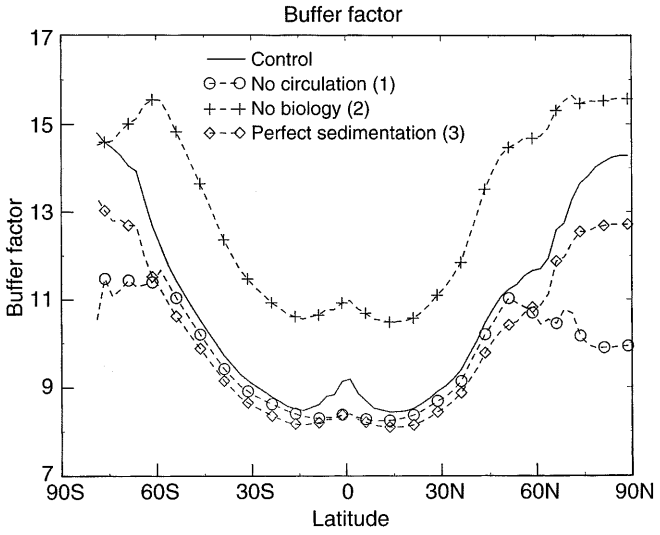

Fig. 5. Zonal average of the buffer factor after 250 years integration for the same experiments as in Fig. 3

4 Experiments with time varying ocean circulation

4.1 The experimental setup

To reach the full potential of the current approach, it is necessary to drive the model with observed (or best guess) CO_2 emissions rather than with observed atmospheric CO_2 concentrations. As the model does not include a terrestrial biosphere component, no perfect match with the observed CO_2 record can be obtained. Given the large uncertainty in the global carbon cycle budget (missing sink discussion) a perfect fit is not the goal of the current work.

The model was started in 1750 spun up to a steady state with an pCO_2 of 276.7 ppm. From 1750 emissions were prescribed following Marland and Boden (1991). From 1989 onward an increase of 1%/year was assumed. In one experiment the feedback of greenhouse gas concentrations on the ocean was suppressed, thus essentially repeating the standard type of estimate of future CO_2 concentrations with fixed ocean circulation (NOFEED). In the other experiment, starting from the same initial conditions, the feedback of atmospheric pCO_2 on ocean circulation was included (FEED). The differences between the two experiments thus gave an estimate of the strength of the potential feedback mechanisms.

In experiment NOFEED the atmospheric pCO_2 increases from approximately 277 ppm in the preindustrial steady state to a 363 ppm in year 1990. This is slightly higher than the observed value of 355 ppm. The agreement must be considered to be good, given the uncertainty in the effective role of the terrestrial biosphere and the potential errors in the prescribed fluxes. In year 2100, the model predicts, with the prescribed emission scenario, an atmospheric pCO_2 of 734 ppm. This represents an increase in atmospheric pCO_2 by a factor of 2.6 compared to the preindustrial steady state of the control run CTRL.

4.2 Changes in ocean circulation

The experiment with atmospheric feedback shows in response to the increase of the atmospheric pCO_2 a marked warming at the surface. The time evolution of this warming is shown for the globally averaged SST in Fig. 6. In year 2000, the SST has warmed by about 0.8 °C compared to the initial state. The warming trend is rapidly increasing through the 21st century due to the faster rate of increase of pCO_2 in the atmosphere (and thus the radiative forcing). Due to the inertia of the system, the response is delayed. In year 2100, the sea surface of the ocean has warmed by 3 °C on average. The pattern of the annual mean SST response is shown in Fig. 7. The warming is strongest in low-latitudes, where the thermal inertia is smallest due to the shallow mixed-layer depths. In high-latitudes areas of little warming or even a slight cooling can be seen south of Greenland, in the Weddell Sea and in the North Pacific. In permanently sea ice covered areas like the central part of the Arctic, the temperature stays at the freezing point and the temperature response is basically zero. The temperature response is rather similar to the results of the coupled ECHAM1/LSG coupled OAGCM (see Fig. 1 in Mikolajewicz et al. 1994). The GFDL coupled model by Manabe et al. (1991) shows no cooling in SST, but shows distinct minima of the warming in the northern North Atlantic and in the Southern Ocean. The global mean net oceanic heat uptake at this time in the present model is about 0.6 PW. The time series of the Northern Hemisphere ice volume (Fig. 8a) shows a dramatic retreat of the sea ice due to the warming.

The changes in the physical circulation are rather similar to the changes in fully coupled OAGCM (Cubasch et al. 1992, see also Mikolajewicz et al. 1994). In the Atlantic, the maximum overturning rate is reduced from 25 to 21 Sv, while the outflow of NADW across 30°S which indicates the strength of the model conveyor belt, is reduced from 20 to 18 Sv, displayed sche-

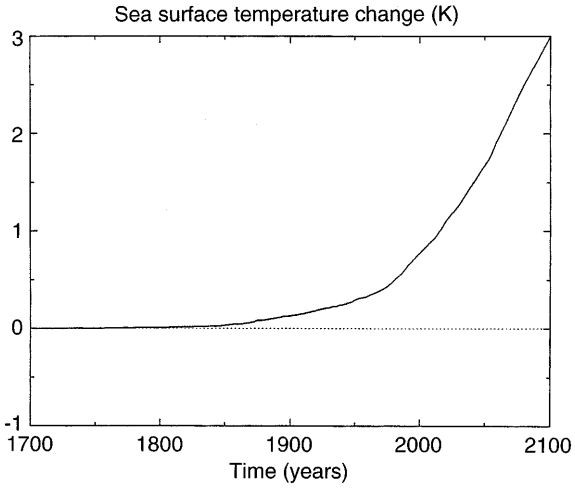

Fig. 6. Time series of global mean SST in experiment FEED relative to the steady state of the spinup

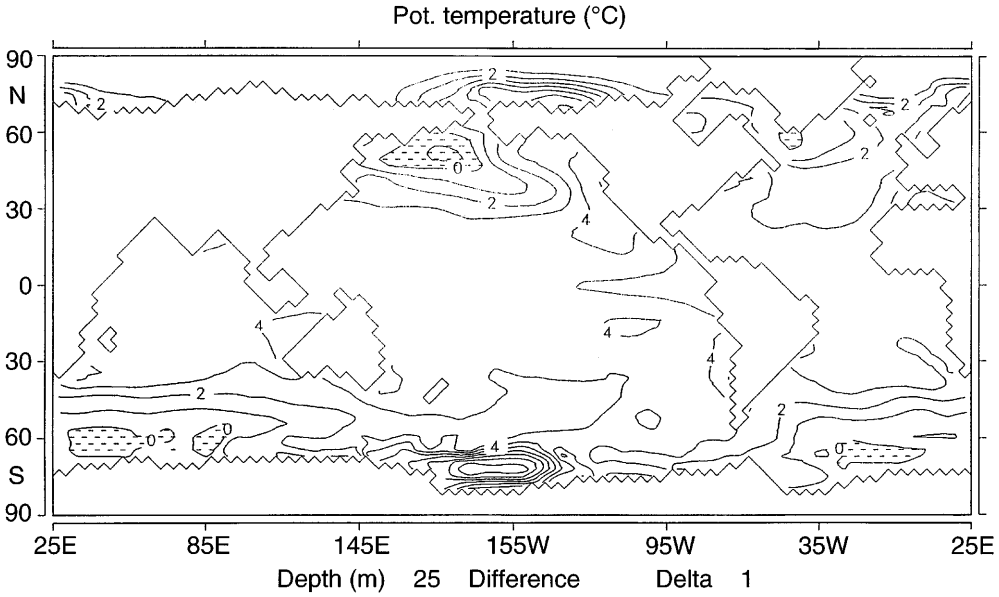

Fig. 7. Change of sea surface temperature at the end of experiment FEED. Contour interval is 1 K, *areas* of cooling are *stippled*

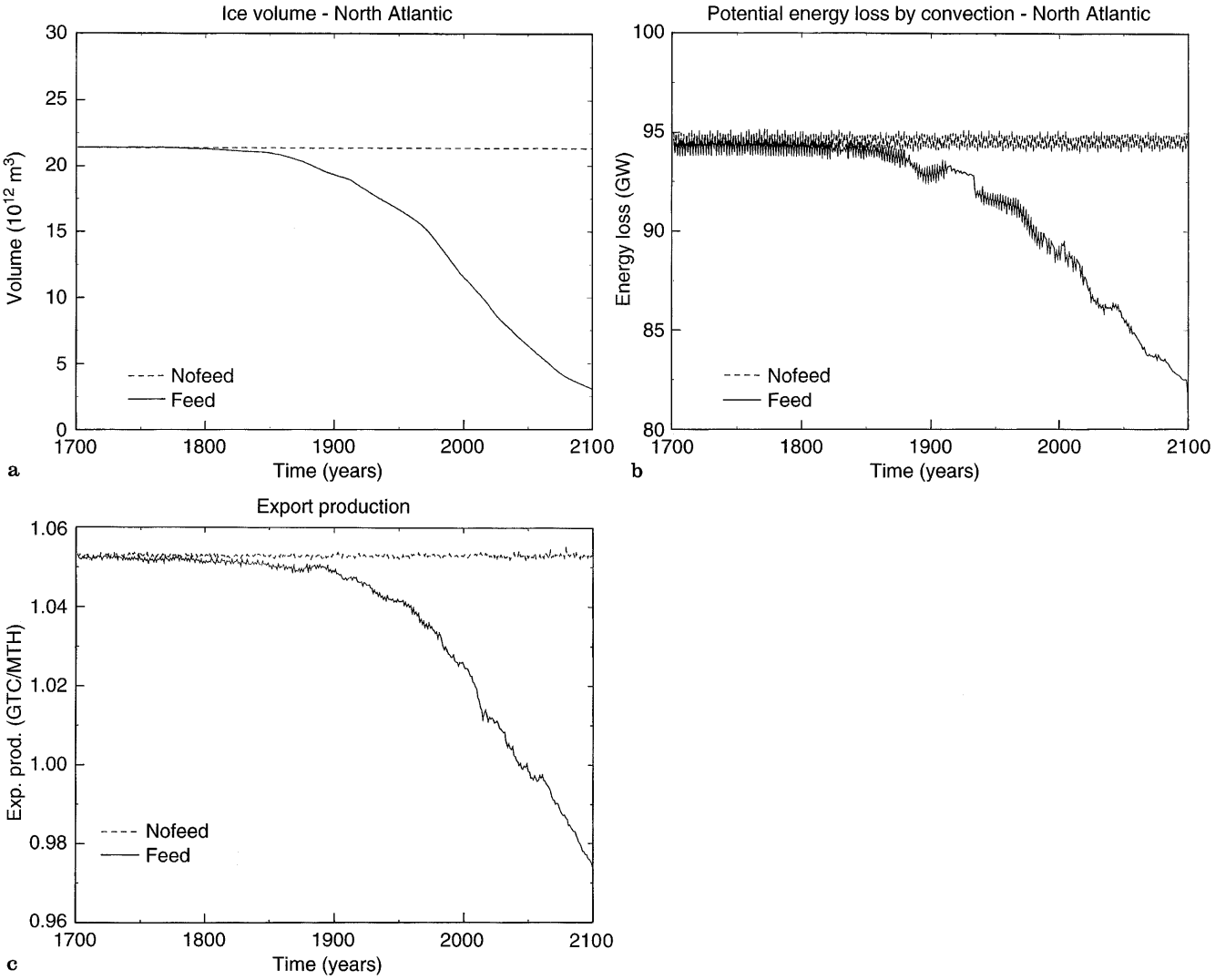

Fig. 8. a Evolution of annual mean Arctic sea ice volume for the experiment with atmospheric CO_2 feedback (FEED, *solid*) and for the experiment without atmospheric CO_2 feedback (NOFEED, *dashed*). **b** Convective release of potential energy for the same experiments. **c** Global export production for the two experiments

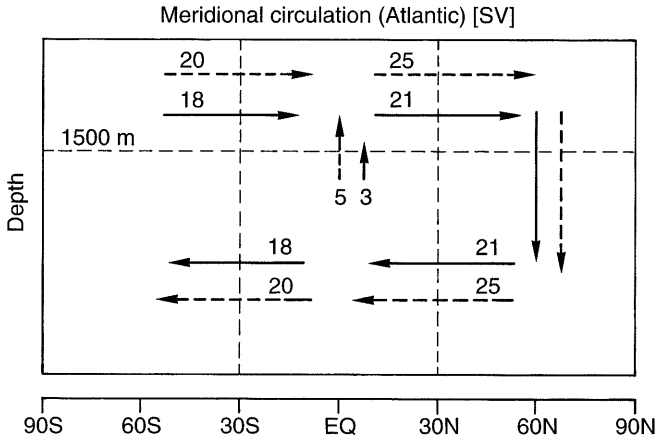

Fig. 9. Atlantic overturning circulation in year 2100 for the experiment with atmospheric CO_2 feedback (FEED, *solid*) and for the experiment without atmospheric CO_2 feedback (NOFEED, *dashed*). The transport between the ocean boxes is given in Sverdrup ($1\ Sv = 10^6\ m^3\ s^{-1}$)

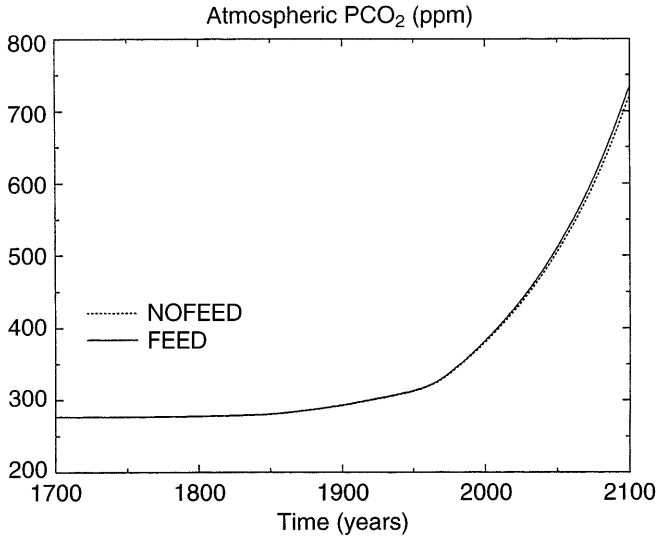

Fig. 10. Evolution of atmospheric pCO_2 for the experiment with atmospheric CO_2 feedback (FEED, *solid*) and for the experiment without atmospheric CO_2 feedback (NOFEED, *dashed*). In year 2100 the atmospheric pCO_2 is increased in the NOFEED experiment to 734 ppm and in the FEED experiment in year 2100 is 13 ppm

matically in Fig. 9. In the coupled OAGCM the the overturning at 30°N was reduced by about 20% in the decade centered around 2080. The outflow of NADW to the Southern Ocean at 30°S is reduced by less than 2 Sv. The absolute strength of the weakening of the Atlantic thermohaline overturning is also in reasonable agreement with the results from the GFDL coupled OAGCM (Manabe et al. 1991). However, the relative reduction of the overturning in their model is significantly larger as their model has a much weaker conveyor-belt circulation (at the time of CO_2 doubling around year 70 of their integration, thus somewhat earlier than the periods discussed for the other models, the overturning at 30°N is reduced from about 16 Sv to roughly 12 Sv, estimated from their Fig. 32).

Since we did not assume a change of the wind field patterns, the surface circulation including Ekman transport induced upwelling is almost unchanged. Figure 8 displays a time series of the most sensitive physical quantities which are the Arctic ice volume (panel a) and the loss of potential energy by convection at places of unstable stratification (panel b). The latter has often been used as a proxy for actual formation rate of NADW (e.g., Mikolajewicz et al. 1990; Mikolajewicz and Maier-Reimer 1994) and thus the driving force of the conveyor belt circulation. It operates primarily outside the ice covered area and is, thus, relatively less reduced (by 13%) than the sea ice volume which at the end of the experiment has almost completely vanished. The locations of deep water formation in this run show a clear tendency to follow the ice edge, which results in a poleward shift of the areas of deep convection. The reduction of overturning also leads to a decrease of the global export production (panel c) by 7.5%. This can be explained mostly by decreased upwelling of nutrients in the tropics due to increased vertical stability.

4.3 Changes of oceanic CO_2 uptake in response to changes in ocean circulation

The effect of the changing ocean circulation on the oceanic CO_2 uptake are small. Figure 10 shows the predicted atmospheric pCO_2 for the two experiments with and without atmospheric feedback (FEED and NOFEED). The temperature feedback leads to a slightly higher atmospheric pCO_2 in experiment FEED, but in the scaling of the Fig. 10, they are almost indistinguishable. The difference at the end of the next century is 13 ppm or 26 GtC, representing a change of only 3% of the total increase.

The corresponding difference in the ocean is quite inhomogeneously distributed. Near the surface, the difference is obviously determined by thermodynamic effects. Since the water in the feedback experiment is warmer by 3 K, the solubility is reduced and the concentration of DIC in surface waters is lower despite the higher pCO_2 in the atmosphere. Since the difference evolves at an atmospheric level above 700 ppm, the thermodynamic effect acts slightly more strongly than in the present ocean, where the sensitivity is approximately 11 ppm/K (see Heinze et al. 1991).

Table 2 gives an overview of changes in the ΣCO_2 pools of the two experiments. The total amount of ΣCO_2 increases in the NOFEED experiment from 1750 to 2100 in the Arctic Ocean by about 3%. The total carbon content in the surface and intermediate waters of the Atlantic (excluding the Arctic Ocean) increased during this period in the surface and intermediate waters by about 5% or nearly 35 GtC and the deep sea by about 3% (32 GtC). Corresponding changes in the Central and Southern Atlantic are much

Table 2. ΣCO_2 pools in GtC of the Atlantic and World Ocean for the experiment without atmospheric CO_2 feedback (NOFEED) in year 1770 and year 2100, and for the experiment with atmospheric CO_2 feedback (FEED). The surface and intermediate ocean boxes are extended from the surface to the 1500 m level, the deep ocean boxes from 1500 m to the bottom. The Arctic Ocean includes the Greenland and Norvegian Sea and is limited on the Pacific side by the Bering Street. The North Atlantic box is extended to 30°N, and the Central Atlantic to 30°S

		NOFEED year 1750	NOFEED year 2100	FEED year 2100
Arctic Ocean	surface + intermediate	455.8	471.5	475.3
	deep	207.0	214.0	211.7
North Atlantic	surface + intermediate	751.8	786.6	784.5
	deep	972.5	1004.8	1001.0
Central Atlantic	surface + intermediate	1749.0	1794.3	1791.0
	deep	3061.0	3103.6	3102.2
South Atlantic	surface + intermediate	1111.6	1140.5	1139.9
	deep	1919.3	1946.3	1945.6
Atlantic Total		10228.1	10461.6	10451.1
World Ocean		38364.5	38920.3	38895.7

smaller (1% in the upper part and 3% in the deep sea). The North Atlantic thus acts as a strong sink for the emitted anthropogenic CO_2. The total increase of ΣCO_2 in the Atlantic is 556 GtC which is about 42% of the world oceans uptake.

The most significant changes between the experiments FEED and NOFEED take place in the surface and intermediate waters of the Arctic Ocean. Here, the reduction of the sea ice cover allows an additional gas exchange in the FEED experiment and increases, together with the higher atmospheric pCO_2, the uptake of carbon relative to the NOFEED experiment by 24%, while in the deep Arctic Ocean the uptake is reduced by 32% due to the weakening in the convection. In the central und southern parts of the Atlantic the increase of the pCO_2 due to the warming effects dominates over the effect of higher atmospheric pCO_2. In the surface and intermediate waters of the other parts of the world ocean, the change in carbon inventory is typically lower in the FEED experiment compared to run NOFEED. The reduction of the formation of NADW and the consecutive slowing down of the thermohaline circulation lead to a reduction of the carbon uptake in the deep North Atlantic by 12% in experiment FEED. In the other parts of the deep sea, the structure of the difference between the two experiments is less obvious.

As a consequence of the reduction in the upwelling of nutrients (mostly in the tropics), the monthly mean export production is reduced from 1.05 to 0.97 GtC. This reduction is lagged by approximately 20 years by a corresponding reduction of upwelling of remineralized organic matter.

The weakening of the thermohaline overturning reduces the speed of sequestering anthropogenic carbon in the deep ocean. However, the release of CO_2 due to the reduced solubility caused by a CO_2 induced warming at the surface dominates the effect of a reduced biological pump by far. The modifications of the CO_2 uptake due to the global warming is, at least on the time scales considered here, much smaller even than the error bars which have to be put on the future oceanic uptake of anthropogenic carbon. A rigorous discrimination between the two opposing effects could be achieved from a simultaneous analysis of changes in temperature, salinity, phosphate, DIC, and alkalinity, but this goes beyond the scope of this work.

5 Conclusions

We have performed several experiments with a general ocean circulation model coupled online with a model of biogeochemical cycling in the ocean. Since we did not allow for an explicit alteration of the biological activity and since the predicted changes in the ocean circulation are not dramatic, the potential feedbacks during the next century are expected to be small. Our findings may be summarized by the following statements:

1. Although biology does not transport directly anthropogenic CO_2 to the deep sea, it causes changes in the inorganic aspects of marine chemistry which have an effect on the gradual uptake of CO_2 by the ocean.

2. We expect the feedbacks to be so small that the currently used modelling strategy of first using a carbon cycle model for the transformation of anthropogenic emissions into pCO_2 and subsequently using the output as forcing for a physical climate model, appears to be justified.

Acknowledgements. We appreciated fruitful discussions with W. Broecker, M. Heimann, C. Heinze, and K. Six. S. Schultz helped to make the plots. Part of the work was supported by EC project EV5V-CT92-0124.

References

Archer D, Maier-Reimer E (1994) Effect of deep-sea sedimentary calcite preservation on atmospheric CO_2 concentration. Nature 367:260–263

Bacastow R (1981) Numerical evaluation of the evasion factor. In: Bolin B (ed) SCOPE 16, Carbon cycle modelling. J. Wiley & Sons Chichester, pp 95–101

Bacastow R, Maier-Reimer E (1990) Ocean-circulation model of the carbon cycle. Clim Dyn 4:95–125

Broecker W (1991) Keeping glocal change honest. Glob Biogeochem Cycles

Broecker WS, Takahashi T (1977) Neutralization of fossil fuel carbon dioxide by marine calcium carbonate. In: Anderson NR, Malahoff A (eds) The fate of fossil fuel carbon dioxide in the Oceans. Plenum Press

Broecker WS, Peng TH (1986) Carbon cycle 1985: glacial to interglacial changes in the operation of the global carbon cycle. Radiocarbon 28:309–317

Broecker WS, Peng TH (1992) Interhemispheric transport of carbon dioxide by ocean circulation. Nature 356:587–589

Bryan F (1986) High-latitude salinity effects interhemispheric thermohaline circulations. Nature 305:301–304

Cubasch U, Hasselmann K, Hoeck H, Maier-Reimer E, Mikolajewicz U, Santer BD, Sausen R (1992) Time-dependent greenhouse warming computations with a coupled ocean-atmosphere model. Clim Dyn 8:55–69

Cubasch U, Santer BD, Hellbach A, Hegerl G, Höck H, Maier-Reimer E, Mikolajewicz U, Stössel A, Voss R (1994) Monte Carlo climate change forecasts with a global coupled ocean-atmosphere model. Clim Dyn 10:1–19

Frankignoulle M, Canon C, Gattuso JP (1994) Marine calcification as a source of carbon dioxide: positive feedback of increasing atmospheric CO_2. Limnol Oceanogr 39:458–462

Gates WL, Mitchell JFB, Boer GJ, Cubasch U, Meleshko VP (1992) Climate modelling, climate prediction and model validation. In: Houghton JT, Callander BA, Varney SK (eds) Climate change 1992. Cambridge University Press Cambridge, UK, pp 97–134

Häder D-P (1993) Effects of enhanced solar ultraviolet radiation on aquatic ecosystems. In: Tevini M (ed), UV-B radiation and ozone depletion. Lewis, Boca Raton

Hasselmann K, Sausen R, Maier-Reimer E, Voss R (1993) On the cold start problem in transient simulations with coupled atmosphere-ocean models. Clim Dyn 9:53–61

Heinze C, Maier-Reimer W, Winn K (1991) Glacial pCO_2 reduction by the World Ocean: experiments with the Hamburg carbon cycle model. Paleoceanography 6:395–430

Houghton JT, Jenkins GJ, Ephraums JJ (1990) Climate change, The IPCC Scientific Assessment. Cambridge University Press, New York

Jones PD, Wigley TML, Wright PB (1986) Global temperature variations between 1861 and 1984. Nature 322:430–434

Levitus S (1982) Climatological atlas of the World Ocean. NOAA Prof Pap 13. Rockville, Maryland 173 pp

Maier-Reimer E (1993) Geochemical cycles in an OGCM. Part I: preindustrial tracer distributions. Glob Biogeochem Cycles 7:645–677

Maier-Reimer E, Hasselman K (1987) Transport and storage of carbon dioxide in the ocean – an inorganic ocean-circulation carbon cycle model. Clim Dyn 2:63–90

Maier-Reimer E, Mikolajewicz U, Hasselmann K (1993) Mean circulation of the Hamburg LSG OGCM and its sensitivity to the thermohaline surface forcing. J Phys Oceanogr 23:731–757

Manabe S, Spelman MJ, Stouffer RJ (1991) Transient responses of a coupled ocean-atmosphere model to gradual changes of atmospheric CO_2. Part I: annual mean response. J Clim 4:785–818

Marland G, Boden TA (1991) CO_2 emissions – modern record. In: Boden TA, Sepanski RJ, Stoss FW (eds) Trends '91: a compendium of data on global/change. ORNL/CDIAC-46, pp 386–507

Mikolajewicz U, Maier-Reimer E (1994) Mixed boundary conditions in ocean general circulation models and their influence on the stability of the models conveyor belt. J Geophys Res 99 (C11):22633–22644

Mikolajewicz U, Sander BD, Maier-Reimer E (19980) Ocean response to greenhouse warming. Nature 345:589–593

Mikolajewicz U, Cubasch U, Hegerl G, Höck H, Maier-Reimer E, Santer BD, Schultz S (1994) Changes in the ocean circulation of the North Atlantic due to an increase of atmospheric greenhouse gas concentrations. ICES Mar Sci Symp 198:292–296

Najjar RG, Sarmiento JL, Toggweiler JR (1992) Downward transport and fate of organic matter in the ocean: simulations with a general circulation model. Glob Biogeochem Cycles 6:45–76

Neftel A, Oeschger H, Schwander J, Stauffer B, Zumbrunn R (1982) Ice core sample measurements give atmospheric CO_2 content during the past 40000 y. Nature 295:220–223

Oescher H, Siegenthaler U, Schotterer U, Gugelmann A (1975) A box diffusion model to study the carbon dioxide exchange in nature. Tellus 27:168–192

Rahmstorf S (1994) Rapid climate transitions in a coupled ocean-atmosphere model. Nature 372:82–85

Revelle R (1985) The scientific history of carbon dioxide. In: Sundquist ET, Broecher WS (eds) The carbon cycle and atmospheric CO_2: natural variations archean to present. AGU Monogr 32, pp 1–4, Washington

Revelle R, Suess HE (1957) Carbon dioxide exchange between atmosphere and ocean and the question of an increase of atmospheric carbon dioxide during the past decades. Tellus 9:18–27

Riebesell U, Wolf-Gladrow DA, Smetacek V (1993) Carbon dioxide limitation of marine phytoplankton growth rates. Nature 361:249–251

Sanyal A, Hemming NG, Hanson GN, Broecker WS (1995) Evidence for a higher pH in the glacial ocean from boron isotopes in foramifera. Nature 373:234–236

Sarmiento JL, Orr JC, Siegenthaler U (1992) A perurbation simulation of CO_2 uptake in an ocean general circulation model. J Geophys Res 97(C3):3621–3645

Siegenthaler U (1983) Uptake of excess carbon dioxide by an outcrop – diffusion model of the ocean. J Geophys Res 88(C6):3599–3608

Takahashi T, Olafson J, Goddard JG, Chipman DW, Sutherland SC (1993) Seasonal variation of CO_2 and nutrients in the high-latitude surface oceans: a comparative study. Glob Biogeochem Cycles 7:843–878

Tziperman E, Toggweiler JR, Feliks Y, Bryan K (1994) Instability of the thermohaline circulation with respect to mixed boundary conditions: is it really a problem for realistic models? J Phys Oceanogr 24:217–232

Winguth A, Heimann M, Kurz K, Maier-Reimer E, Mikolajewicz U, Segschneider J (1994) El Niño-Southern Oscillation related fluctuations of the marine carbon cycle. Glob Biogeochem Cycles 8:39–63

Wolf-Gladrow D (1994) The ocean as part of the global carbon cycle. Environ Sci Pollut Res 1:99–106

Wright DG, Stocker TF (1993) Younger Dryas experiments. In: Peltier WR (ed) Ice in the climate system. pp 395–416

Zhang S, Greatbatch RJ, Lin CA (1993) A reexamination of the polar halocline catastrophe and implications for coupled ocean-atmosphere modelling. J Phys Oceanogr 23:287–299